THE JOURNAL OF PHYSICAL CHEMISTRY B

Article

pubs.acs.org/JPCB

The Stability of Bisulfite and Sulfonate Ions in Aqueous Solution Characterized by Hydration Structure and Dynamics

Viwat Vchirawongkwin,*[,†] Chokchai Pornpiganon,[†] Chinapong Kritayakornupong,[‡] Anan Tongraar,[§] and Bernd M. Rode[⊥]

[†]Department of Chemistry, Faculty of Science, Chulalongkorn University, Phayathai Road, Patumwan, Bangkok 10330, Thailand

[‡]Department of Chemistry, Faculty of Science, King Mongkut's University of Technology Thonburi, Bangkok 10140, Thailand

[§]School of Chemistry, Institute of Science, Suranaree University of Technology, Nakhon Ratchasima 30000, Thailand

[⊥]Theoretical Chemistry Division, Institute of General, Inorganic and Theoretical Chemistry, University of Innsbruck, Innrain 52a, A-6020 Innsbruck, Austria

ABSTRACT: The aqueous solutions of bisulfite (SO_3H^-) and sulfonate (HSO_3^-) were simulated by the ab initio quantum mechanical charge field molecular dynamics (QMCF MD) formalism. All superimposed trajectories for the atomic coordinates of solutes with three-dimensional alignment here illustrated the reactivities of the ions. Power spectra were evaluated on the basis of the velocity autocorrelation functions (VACFs) with the normal-mode analysis, presenting a higher frequency of the symmetric SO_3 deformation ($\delta_s(SO_3)$) than the asymmetric SO_3 deformation ($\delta_{as}(SO_3)$) modes for the sulfonate ion. The different influence of solvent on the frequency of the O−H and S−H stretching suggests a higher stability of hydrated sulfonate ion. The bisulfite shows a slightly stronger molecular hydration shell than the sulfonate ion with the average number of ion−solvent hydrogen bonds (H-bonds) of 5.3 and 5.0, respectively. Extra water molecules within the molecular hydration shell are found for bisulfite (1.2) and for sulfonate (1.6). The mean residence times for the water ligands classify each ion as a structure maker, while the S−H bond within the sulfonate ion displays a hydrophobic behavior. No tautomerization was observed within the simulation period.

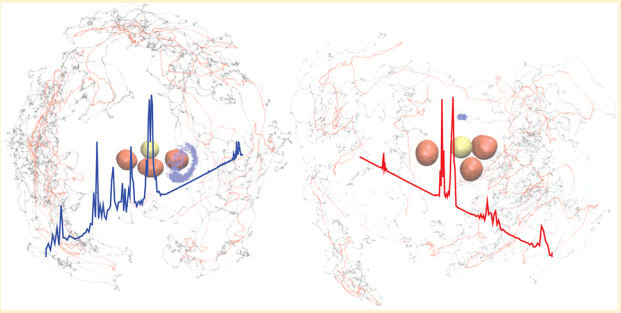

INTRODUCTION

The man-made emissions of sulfur dioxide (SO_2) in the atmosphere are one of the serious air pollutions;[1] however, the winemaking process uses SO_2 to inhibit the growth of indigenous yeasts and contaminating bacteria, and suppress the formation of quinones.[2] The first protonation of dissolved SO_2 in water produces two tautomeric forms, namely bisulfite (SO_3H^-) and sulfonate (HSO_3^-) ions, identified by ultraviolet absorption[3] and Raman[4,5] studies. For the former, the proton attaches to one oxygen atom, whereas the hydrogen in the latter binds to the sulfur atom. The characterization of both ions was reported in many IR and Raman experiments.[4−9] Risberg et al. assigned seven and six frequencies for the bisulfite and sulfonate ion, respectively, via the Raman investigation of 1 M $NaHSO_3$ at pH 3.9.[8] They also assigned the frequency of the symmetric SO_3 deformation ($\delta_s(SO_3)$), lower than the asymmetric SO_3 deformation ($\delta_{as}(SO_3)$), to the sulfonate ion, while the inclusion of the sulfur isotope effect[6] suggested a reversed order. Varying assignments for the O−H stretching mode of the bisulfite ion were also reported from Raman experiments.[7−9] A recent FTIR spectroscopy in conjunction with a laminar flow-tube and the scanning mobility particle sizer measurements was also unable to assign the frequency to all normal modes for both ions.[9]

The oxygen-17 NMR spectroscopy reported the equilibrium quotient for the isomerization reaction between bisulfite and sulfonate ions ($Q = [SO_3H^-]/[HSO_3^-]$) to be 4.9 ± 0.1 at 298 K in solutions of ionic strength 1.0 *m*,[10] while the sulfur K-edge XANES experiment at the total concentration of 0.05 M without ionic medium gave this value as 2.6 ± 0.5.[8] Baird and Taylor[11] utilized the single-determinant SCF with a small basis set obtaining a more stable sulfonate than bisulfite ion by 5 kcal mol^{-1}, while the superior MC-SCF with double-ζ basis set predicted the bisulfite to be the more stable isomer.[12] The MP2 and MP4 calculations with a 6-31++G(d,p) basis set reported a higher stability of the bisulfite by approximately 8 kcal mol^{-1} compared to the sulfonate ion in the gas phase.[13] The theoretical results including small water clusters also indicated that the bisulfite ion is more stable than the sulfonate ion.[14] Calculations at the G2 and G2(MP2) level with the inclusion of multiple polarization functions on the sulfur atom indicated

Received: June 9, 2012
Revised: August 24, 2012
Published: August 25, 2012

   dx.doi.org/10.1021/jp305648e | *J. Phys. Chem. B* 2012, 116, 11498−11507

that the sulfonate ion is more stable than the bisulfite ion by approximately 4 and 5 kcal mol^{-1} in the gas and aqueous phase, respectively.[15] Otto et al. also concluded a more stable sulfonate ion in the gas phase.[16] The bisulfite with the C_s symmetry has two conformations, namely *cis*- and *trans*-SO_3H^-, in which the O−H bond is located bisecting and opposite the ∠OSO angle, respectively.[12] Both C_s conformations are the transition state in the gas phase according to the negative eigenvalue in their calculated Hessian matrices; however, the *trans*-SO_3H^- has a higher energy than the *cis*-conformer by about 5 kcal mol^{-1}.[13] Voegele et al. proposed a mechanism of tautomerization from the bisulfite into the sulfonate ions through the *trans*-SO_3H^-.[17]

According to the coexistence of bisulfate and sulfonate ions in equilibrium solutions and other variety of sulfite(IV) species,[1,8,10] their hydration structure has never been characterized in any experiments. Within a computer simulation, we set up aqueous solutions of bisulfite and sulfonate ions to acquire the structural and dynamical of these solutes and their respective hydration shells by means of an ab initio quantum mechanical charge field molecular dynamics (QMCF MD) formalism[18,19] to compare the stability for both ions in the environment of explicit water molecules. We evaluated the vibrational frequencies for all normal modes of both ions based on a precise vector analysis, and also investigated the role of water molecules within the hydration shell on the strength of chemical bonds.

METHODS

In order to investigate the structural and dynamical properties of solutes and their hydration shell, we have applied the ab initio quantum mechanical charge field molecular dynamics (QMCF MD) formalism.[18,19] This method avoids the construction of potential functions between the solute and water molecules in bulk by extending the quantum mechanically treated solvent layer beyond the first hydration shell of the solute species, resulting in negligible non-Coulombic interactions between the solute and bulk water.[20−23] The involvement of the point charges of the atoms in the molecular mechanical (MM) region with their changing positions in the core Hamiltonian for the quantum mechanical (QM) calculations is a valuable feature of this method with a perturbation term as

$$V' = \sum_{i=1}^{n}\sum_{j=1}^{m}\frac{q_j^{\mathrm{MM}}}{r_{ij}} \tag{1}$$

where n is the number of atoms in the QM region, m is the number of atoms in the MM region, q_j^{MM} is the partial charges of these atoms according to the selected water model, and r_{ij} refers to the distance between a pair of particles in the QM (i) and MM (j) regions. On the other hand, the dynamically changing charges of QM particles, q_i^{QM}, determined by population analysis contribute to the force on each atom j in the MM region as Coulombic forces,

$$F_j^{\mathrm{QM}\rightarrow\mathrm{MM}} = \sum_{i=1}^{n}\frac{q_i^{\mathrm{QM}}\cdot q_j^{\mathrm{MM}}}{r_{ij}} \tag{2}$$

The QMCF MD method permits the migration of water molecules between the QM and MM region by including a smoothing function,[24]

$$S(r) = \begin{cases} 1 & \text{for } r < r_{\mathrm{on}}, \\ \dfrac{(r_{\mathrm{off}}^2 - r^2)^2(r_{\mathrm{off}}^2 + 2r^2 - 3r_{\mathrm{on}}^2)}{(r_{\mathrm{off}}^2 - r_{\mathrm{on}}^2)^3} & \text{for } r_{\mathrm{on}} \le r \le r_{\mathrm{off}}, \\ 0 & \text{for } r > r_{\mathrm{off}} \end{cases} \tag{3}$$

where r is the distance of a given solvent molecule from the center of the simulation box, r_{off} is the radius of the QM region and r_{on} is the inner border of the smoothing region. In this way, one applies this function to all atoms of molecules located in the smoothing region to ensure a continuous transition and change of forces for these molecules according to

$$F_j^{\mathrm{smooth}} = F_j^{\mathrm{MM}} + (F_j^{\mathrm{layer}} - F_j^{\mathrm{MM}}) \times S(r) \tag{4}$$

where F_j^{layer} is the force acting on a particle j located in the (outer QM) smoothing zone and F_j^{MM} is the force acting on a particle j in the MM region. In this context, it has to be mentioned that energy is not rigorously conserved, but the related error due to the short simulation time and the large size of the QM region can be considered extremely minor.

The systems consisted of 495 water molecules with one bisulfite and one sulfonate anion in the bisulfite and sulfonate solution, respectively, in a cubic box of 24.66 Å with periodic boundary condition. The simulations performed in the canonical ensemble using a general predictor-corrector algorithm with a time step of 0.2 fs. We applied the Berendsen temperature-scaling algorithm[25] to maintain the temperature of systems at 298.16 K with a relaxation time of 100 fs. Although this temperature-scaling algorithm requires, in principle, a long simulation period to describe the phase space sufficiently, a large number of successful publications of QMCF MD simulations[26−33] indicate that the simulation period of 10 ps is adequate to reproduce the properties of hydrated ions well. The density of the simulation boxes was 0.997 g cm^{-3}, as the experimental value of pure water at 298 K. The QM subregions, namely the core and layer zones, extended for both bisulfite and sulfonate anions to 3.5 and 6.0 Å, respectively. The structural and dynamical results obtained from previous QMCF MD studies[26−33] have also indicated the Hartree−Fock (HF) method to be a decent compromise between accuracy and affordable computational effort; thus, we also utilized the quantum mechanical calculation at the HF level with the Dunning double-ζ plus polarization (DZP)[34,35] basis sets for hydrogen and oxygen atoms of water molecules and the Dunning double-ζ plus polarization and diffuse functions (DZP +)[34,35] basis sets for hydrogen, oxygen, and sulfur atoms of both bisulfite and sulfonate anions. Although HF and the methodical problems associated with the thermostat probably led to slightly underestimated values of H-bond energies, the associated errors are probably within a 10% range.[33] The thickness of the smoothing region was 0.2 Å with the values of r_{on} and r_{off} respectively as 5.8 and 6.0 Å, according to the radial distribution functions (RDFs) obtained from the equilibrated simulations. In QMCF MD formalism, we utilized the flexible BJH−CF2 water model[36,37] to calculate the interactions between pairs of water in the MM region, with the cutoff distances of 3.0 and 5.0 Å for non-Coulombic interactions between H atoms and between O and H atoms, respectively. This water model supports the fully flexible geometries of water molecules transiting between the QM and MM region and uses the partial charges for oxygen and hydrogen atoms of −0.65966

dx.doi.org/10.1021/jp305648e | J. Phys. Chem. B 2012, 116, 11498−11507

and +0.32983, respectively. The Coulombic interactions between the Mulliken charges on the atoms within the QM region and the point charges of water molecules according to the BJH−CF2 model provide electrostatic forces described by a dynamical field of point charges, which vary according to the movements of atoms inside the QM region and water molecules in the MM region during the simulation. This ensures the continuous adaptation of the Coulombic interactions to all polarization and charge-transfer effects within the solute and surrounding solvent layers.[18,19] In addition, the reaction field method combined with the shifted-force potential technique accounted for the long-range electrostatic potentials and forces within the systems, with a spherical cutoff limit of 12.350 Å. We equilibrated the systems with the QMCF MD method for 50,000 steps (10 ps), and collected further 50,000 steps (10 ps) as data sampling for analyzing the structural and dynamical properties. The average number of water molecules in the QM region was 24.7 and 23.6 for the bisulfite and sulfonate solution, respectively.

In this work, we evaluated the structural and dynamical properties for the hydration shell of bisulfite and sulfonate anions in both individual and molecular manners such as the molecular RDFs, molecular coordination number distributions (CNDs), and molecular ligand mean residence times (MRTs). The definition of the molecular hydration shell is the combination of all atomic hydration spheres for each anion, producing the molecular domain.[38] The coordinating site for each water molecule to the anions is the shortest distance between the oxygen atom of a water molecule and each atom within each anion.[31,33] We calculated all MRT values on the basis of direct method,[39] counting the water exchange processes between hydration shell and bulk. The most appropriate time span to record a water displacement from its original coordination sphere as an exchange process is 0.5 ps,[39,40] which corresponds to the average lifetime of a hydrogen bond in the solvent.[41]

The velocity autocorrelation function (VACF) is one method to evaluate the dynamical properties of a fluid system related to macroscopic transport coefficients, and its Fourier transformation yields the vibrational spectrum via normal-coordinate analysis.[42] The definition of normalized VACF, $C(t)$, is

$$C(t) = \frac{\sum_i^{N_t} \sum_j^{N} v_j(t_i) v_j(t_i + t)}{N_t N \sum_i^{N_t} \sum_j^{N} v_j(t_i) v_j(t_i)} \quad (5)$$

where N is the number of particles, N_t is the number of time origins t_i, and v_j denotes a certain velocity component of the particle j. A correlation length of 2.0 ps was used to obtain the power spectra with 4000 averaged time origins.

RESULTS AND DISCUSSION

Structural and Dynamical Properties of Solutes. According to the molecular dynamics protocol, all atoms in the simulation box move along the gradient of forces during the simulation period. Thus, average internal coordinates such as bond distances, angles, and dihedral angles are suitable to represent the geometry of bisulfite and sulfonate ions obtained from the QMCF MD simulations. Nine structural parameters with their statistical deviation used to construct each average geometry of ions are listed in Table 1 and their geometries shown in Figure 1. All S−O distances are shorter than those within SO_3^{2-} of 1.53 Å obtained from QMCF MD and LAXS.[43]

Table 1. Nine Structural Parameters for the Geometry of SO_3H^- and HSO_3^- Ions Obtained from the Averaging of Their Distributions with Their Variations

SO_3H^-		HSO_3^-	
structural parameter		structural parameter	
S−O(1) (Å)	1.50 ± 0.03	S−O(1) (Å)	1.47 ± 0.03
S−O(2) (Å)	1.50 ± 0.03	S−O(2) (Å)	1.47 ± 0.03
S−O(3) (Å)	1.63 ± 0.04	S−O(3) (Å)	1.46 ± 0.02
O(3)−H (Å)	0.98 ± 0.03	S−H (Å)	1.33 ± 0.04
∠O(1)SO(3) (deg)	102 ± 4	∠O(1)SO(2) (deg)	112 ± 3
∠O(2)SO(3) (deg)	102 ± 4	∠O(2)SO(3) (deg)	112 ± 3
∠SO(3)H (deg)	119 ± 7	∠O(1)SH (deg)	106 ± 3
O(1)SO(3)O(2) dihedral (deg)	−111 ± 3	O(2)SO(1)H dihedral (deg)	116 ± 3
O(2)SO(3)H dihedral (deg)	52 ± 67	O(3)SO(2)O(1) dihedral (deg)	−128 ± 4

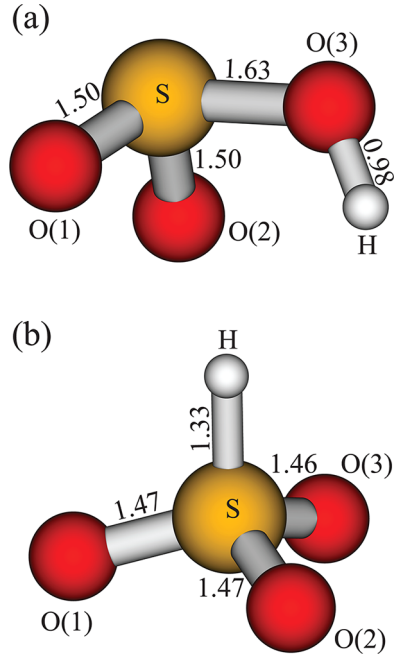

Figure 1. Average geometries of (a) bisulfite (SO_3H^-) and (b) sulfonate (HSO_3^-) ions obtained from the QMCF MD simulations.

Remarkableness is the large variation of the O(2)SO(3)H dihedral angle of 67° within the bisulfite ion, while other angles vary within 7°. However, the interpretation of the data only from the statistical distribution has some limitation. The visualization of the solutes in the simulations period provides more details, but the large number of configurations realized in the dynamics require a specific analysis. Thus, we utilized the superimposed configurations with the three-dimensional (3D) alignment by using the contravariant transformation, representing the dynamical motions of bisulfite and sulfonate ions shown in Figure 2. We defined new basis vectors via the facet constructed from three oxygen atoms for each trajectory configuration. The z-axis is the unit normal vector of the facet, while the unit vector of the vector sum between two vectors of vertices defines the x-axis. The y-axis is the unit normal vector of the cross product between the z- and x-axes. Figure 2a shows the ease of rotations for the hydrogen atom around the S−O(3) bond in bisulfite ion, while Figure 2b presents small motions for all atoms in the sulfonate ion. The small diffusion

dx.doi.org/10.1021/jp305648e | J. Phys. Chem. B 2012, 116, 11498−11507

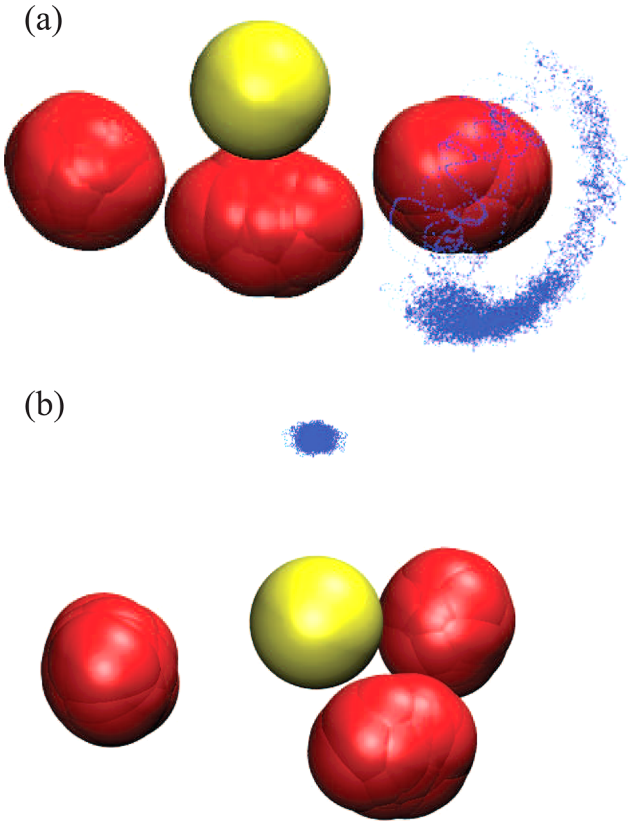

Figure 2. All superimposed trajectories for the coordinates of (a) bisulfite (SO_3H^-) and (b) sulfonate (HSO_3^-) ions with 3D alignment obtained from the QMCF MD simulations. The yellow sphere is the sulfur, red spheres are the oxygen, and blue points are the hydrogens.

of motions for the sulfonate ion indicates a higher kinetic stability of the interaction with its hydration shell than the bisulfite ion, consisting of the active hydrogen atom, rotating around the O(3) atom. These data agree with the XANES results that the number of sulfonate ions increased with increasing temperature.[8] According to the proposed mechanism of tautomerization by Voegele et al.,[17] the hydrogen atom of SO_3H^- aligned in the *trans*-conformer yields the sulfonate ion. This conformer is the transition state in the gas phase, according to its single negative eigenvalue in its calculated Hessian matrix. We also performed G3(MP2) calculations[44] in the polarizable continuum model (PCM) on the *trans*-conformer by using the *Gaussian03* package,[45] obtaining all positive eigenvalues of the calculated Hessian matrix. This reveals the role of solvent to stabilize the energy of *trans*-SO_3H^-, providing the suitable arrangement of water cluster for the tautomerization process.[17] However, the local minimum for the rotamer of SO_3H^- ion is located in between the *cis*- and *trans*-conformers. Its low probability apparently is not sufficient to observe on isomerization reaction within the short time-span of the simulation. In order to investigate the probability of the rotation for the hydrogen atom of bisulfite ion, we defined a new dihedral angle, namely H−O(3)−α−S, where α is the center of the facet constructed from three oxygen atoms, presenting the *cis*- and *trans*-SO_3H^- by ±180° and 0°, respectively. This angle distribution clarified the ratio of conformers by the rotational ability of the hydrogen atom around the S−O(3) bond throughout the simulation period shown in Figure 3. The active forms of bisulfite tend to be the

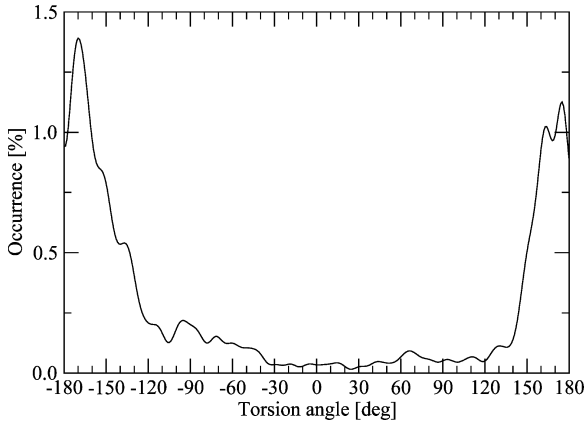

Figure 3. Angle distribution of the O(2)SO(3)H dihedral angle in SO_3H^- ion.

trans-conformer having the H−O(3)−α−S angle in the range from −90° to 90° to be only 12.23%, indicating a reduced probability of conversion to the sulfonate ion based on the proposed mechanism by Voegele et al.[17] This agrees with the equilibrium quotient obtained from the experiments, specifying an excess of bisulfite ion over the sulfonate ion.[8,10]

One dynamical property of the solutes obtained from the QMCF MD simulations comparable to the infrared (IR) and Raman (R) data is the vibrational spectrum. According to the dynamical motions of all atoms within the bisulfite ion, its symmetry is the C_1 consisting of nine vibration modes. We analyzed the normal modes by separating the ion into three bases such as (SO_2), (SO_2)−(O*), and (SO_2O)−(H) models. The (SO_2) part comprises two equivalent S−O bonds assigned with the C_{2v} symmetry consisting of three modes, namely symmetric SO_2 stretching ($\nu_s(SO_2)$), asymmetric SO_2 stretching ($\nu_{as}(SO_2)$), and SO_2 bending ($\delta(SO_2)$). The addition of an oxygen atom to the first part produced the (SO_2)−(O*) model having three additional vibrational modes, defined as S−OH stretching (ν(S−OH)), S−OH bending, and S−OH out-of-plane bending. These two bending modes equal the SO_2 wagging ($\omega(SO_2)$) and SO_2 twisting ($\tau(SO_2)$) modes, respectively, assigned in other works.[8,46] The last three modes, namely O*−H stretching (ν(O*H)), S−O*−H bending (δ(SO*H)), and S−O*−H wagging (ω(SO*H)), occur when attaching the hydrogen atom producing the (SO_2O)−(H) model. Figure 4 displays the defined vectors for all normal modes of the bisulfite ion, and all power spectra are displayed in Figure 5. On the other hand, the sulfonate ion in C_{3v} symmetry, also having nine modes, will span into two types of symmetry species as the following representation:

$$\Gamma(C_{3v}) = 3a_1(R, IR) + 3e(R, IR) \quad (6)$$

predicting only six bands with three of them becoming doubly degenerate modes. Figure 6 presents all power spectra of the sulfonate ion. All frequencies evaluated from the QMCF MD simulations for both ions are shown in Table 2, also presenting the scaled values in parentheses with the factor of 0.902 obtained from the correction with the coupled-cluster singles and doubles (CCSD) level.[27] Three calculated frequencies (without scaling) of the (SO_2) model for the bisulfite ion are higher than the data from the Raman[8] and FTIR[9] experiments within 80 cm^{-1}, while the scaled values around 50 cm^{-1} are too low. The ν(S−OH) is a simple mode as shown in Figure 4, obtained from the projection of velocity for the O(3) atom

dx.doi.org/10.1021/jp305648e | J. Phys. Chem. B 2012, 116, 11498−11507

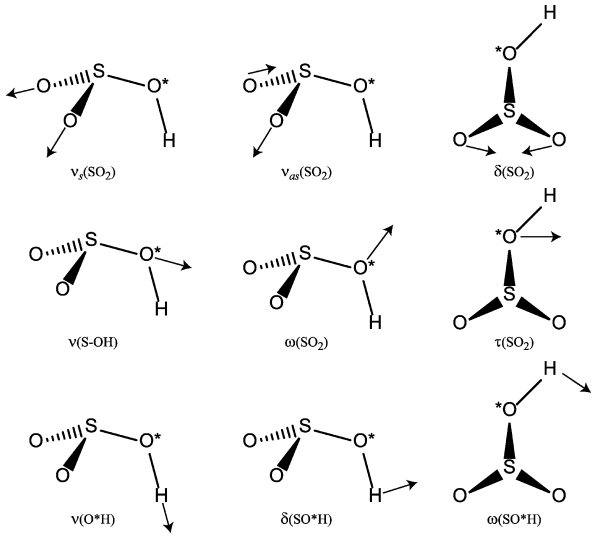

Figure 4. Defined vectors of the normal modes for the SO_3H^- ion in the C_1 symmetry.

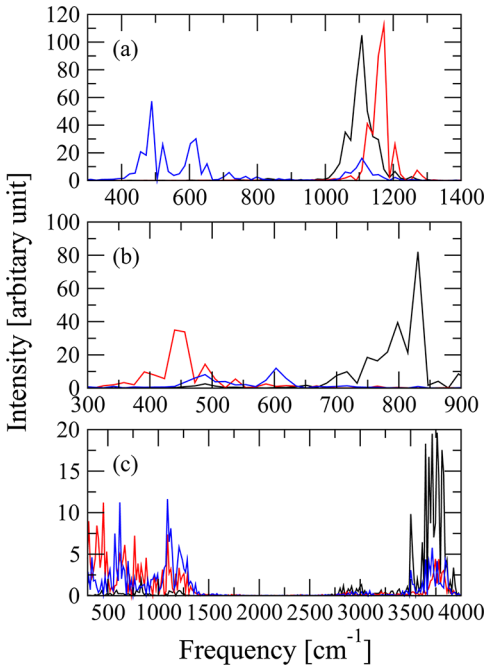

Figure 5. Power spectra of (a) (SO_2) model (black, red, and blue solid lines refer to $\nu_s(SO_2)$, $\nu_{as}(SO_2)$, and $\delta(SO_2)$, respectively), (b) $(SO_2)-(O^*)$ model (black, red, and blue solid lines refer to ν(S−OH), $\omega(SO_2)$, and $\tau(SO_2)$, respectively), and (c) $(SO_2O)-(H)$ model (black, red, and blue solid lines refer to ν(O*H), δ(SO*H), and ω(SO*H), respectively).

onto the S−O(3) vector. The calculated frequency for this mode supports the assignment by Connick et al.[5] at 730 cm^{-1}. The values of more sophisticated modes, $\omega(SO_2)$ and $\tau(SO_2)$, agree with the Raman data reported by Risberg et al.,[8] again indicating a good quality of vector analysis for the normal modes. The spectra of the OH group present very broad bands, due to the different orientation of the O(3)−H bond for each time origin producing the mixed modes as the previous results of HSO_3^- ion.[33] We subtracted one spectrum of O(3)−H from five other spectra, the rest being two modes of $(SO_2O)-(H)$ including three modes from the $(SO_2)-(O^*)$ model, to clarify

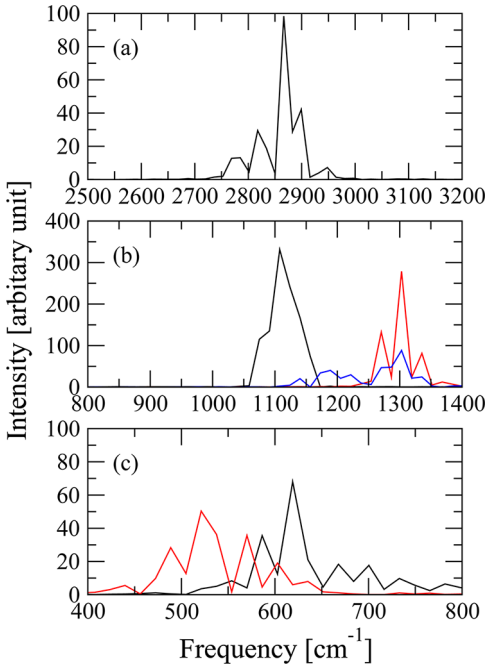

Figure 6. Power spectra of (a) ν(SH) mode, (b) $\nu_s(SO_3)$, $\nu_{as}(SO_3)$, and δ(SH) modes (represented via a black, red, and blue solid line, respectively), and (c) $\delta_s(SO_3)$ (black solid line) and $\delta_{as}(SO_3)$ (red solid line) modes.

the location of the peak for each mode. Figure 7 shows three isolated spectra, obtained from the procedure. The characteristic of the isolated spectrum for ν(O*H) has still the broad band, found in the region of 3486−3974 cm^{-1}, while the remaining two spectra display the same pattern with two main peaks. There are two main peaks of the δ(SO*H) spectrum located at 309 and 880 cm^{-1} and of ω(SO*H) at 570 and 1091 cm^{-1}. To our knowledge, these two modes have never been assigned in the spectra obtained from the experiments.[5,7−9] According to an ambiguous assignment of ν(O*H) mode,[7−9] we again clarified the characteristic frequency of this mode by investigating the influence of water molecules in the hydration shell of the hydrogen atom with a method similar to that used for the bicarbonate ion.[32] We evaluated the number of H-bonds between the hydrogen atom of bisulfite ion and water molecules within its hydration shell during the simulation period shown in Figure 8a, according to the geometric criteria.[32,47] Two short time periods, 1.9−4.4 ps and 4.5−7.0 ps, were selected to evaluate the power spectra of the ν(O*H) mode without and with the effect of H-bonds, respectively. The spectrum without the effect of H-bonds has a strong peak located at 3828 (3453) cm^{-1} and a weak peak at 3762 (3393) cm^{-1}, while the main peaks of the spectrum with the H-bonds are red-shifted to 3746 (3379) and 3648 (3290) cm^{-1}. The weak peak located at 3518 (3173) cm^{-1} also occurs in the latter spectrum, revealing the interaction between the hydrogen atom and water molecules.

The power spectrum of the ν(SH) mode in the sulfonate ion displays a split peak, and we again analyzed the influence of hydration shell with the geometric criteria of H-bonds[32,47] between S−H and oxygen of water shown in Figure 8b. A stronger interaction with solvent molecules is found in the time period of 0.5−2.5 ps, while between 4.6 to 6.6 ps fewer interactions are registered. The spectrum of the ν(SH) mode in each period presents the single strong peak at 2915 and 2867

dx.doi.org/10.1021/jp305648e | J. Phys. Chem. B 2012, 116, 11498−11507

Table 2. Vibration Frequencies (cm^{-1}) of Peaks for Each Normal Mode of SO_3H^- and HSO_3^- Ions Evaluated by the VACFs of QMCF MD Simulations, Given As Values Scaled by the Factor 0.902[27] in Parentheses

SO_3H^-			HSO_3^-		
vibration mode[a]	QMCF MD	Raman and IR	vibration mode[a]	QMCF MD	Raman and IR
$\nu_s(SO_2)$	1108 (999)	1053[b], 1050[c]	ν(SH)	2867, 2932 (2586, 2645)	2535[b], 2573[f]
$\nu_{as}(SO_2)$	1173 (1058)	1095[b]	$\nu_s(SO_3)$	1124 (1014)	1025[b], 1030[c], 1038[f]
$\delta(SO_2)$	619 (558)	582[b]	$\delta_s(SO_3)$	651 (587)	496[b], 626[f]
ν(S−OH)	831 (750)	1082[b], 1090[c], 730[d]	$\nu_{as}(SO_3)$	1303 (1175)	1210[b], 1180[c], 1250[f]
$\omega(SO_2)$	440 (397)	378[b]	δ(SH)	1238 (1117)	1126[b], 1120[c], 1122[f]
$\tau(SO_2)$	603 (544)	432[b]	$\delta_{as}(SO_3)$	521 (470)	648[b], 509[f]
ν(O*H)	3648, 3762 (3290, 3393)	3145[b], 3247[c], 3622[e]			
δ(SO*H)	309 (279)				
ω(SO*H)	570 (514)				

[a]Notation of vibration modes: stretching (ν); bending (δ); twisting (τ); wagging (ω); symmetric (subscript s); asymmetric (subscript as). [b]Raman data of 1 M $NaHSO_3$ at pH 3.9.[8] [c]FTIR data of 1 wt % SO_2 H_2O.[9] [d]Raman data of a dilute solution of bisulfite in 1 M $NaClO_4$ solution at 25 °C.[5] [e]Attenuated total internal reflection (ATR) data of aqueous SO_2 solution at −10 °C.[7] [f]Raman data of $CsHSO_3$.[6]

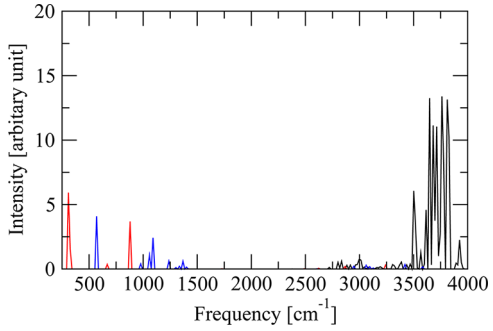

Figure 7. The isolated spectra of ν(S−OH) (black solid line), $\omega(SO_2)$ (red solid line), and $\tau(SO_2)$ (blue solid line) modes for the (SO_2)−(O*) model.

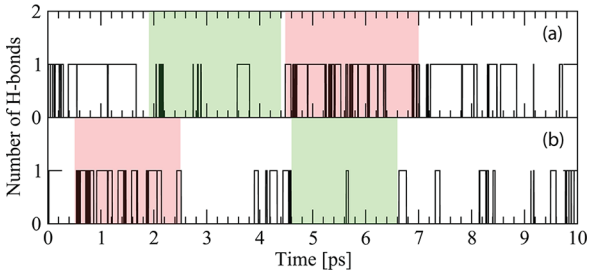

Figure 8. Number of hydrogen bonds between the hydrogen of (a) bisulfite and (b) sulfonate ion and water molecules evaluated by the geometric criteria[32,47] during the simulation period, utilizing short time periods to investigate the effect of H-bonds on the ν(O*H) and ν(SH) frequencies. The selected short time periods with and without the effect of H-bonds are represented by red and green boxes, respectively.

cm^{-1} with and without the effect of water molecules, respectively, specifying a peculiar property of the S−H bond induced by the hydration shell. Steudel et al. reported the blue-shifted peak of ν(SH) by increasing water molecules in a small cluster.[48] Thus, we also investigated the influence of water on the S−H bond with a small model, containing one water molecule interacting on the hydrogen atom of sulfonate ion. HF, MP2, and QCISD calculations with the same basis sets of the QMCF MD simulations were performed on the system with a constrained distance of $S_{sulfonate}\cdots O_{water}$ from 3.50 to 4.50 Å by a step of 0.1 Å solvated in the PCM, by using the *Gaussian 03* package.[45] Figure 9 shows the changing distances of the S−

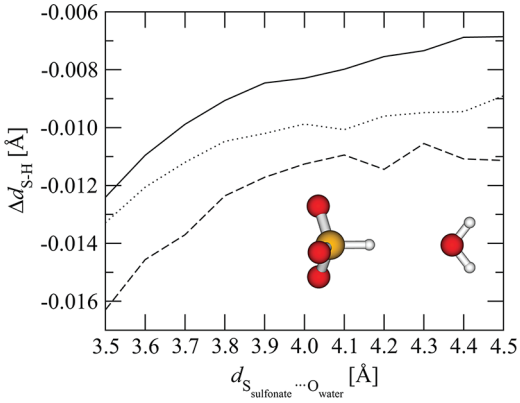

Figure 9. The function between the relative S−H distance with its optimized distance in a single ion calculation at the same theoretical level (Δd_{S-H}) and the distance of $S_{sulfonate}\cdots O_{water}$ ($d_{S_{sulfonate}\cdots O_{water}}$) calculated at the HF (solid line), MP2 (dotted line), and QCISD (dashed line) levels.

H bond affected by the distance of the water molecule. The shorter S−H distance represents a stronger bond and reflects a blue-shifted peak in the spectra, denoting an increased stability of the sulfonate ion in aqueous solution compared to that of the bisulfite ion. The calculated frequencies of $\nu_s(SO_3)$, $\nu_{as}(SO_3)$, and δ(SH) modes agree with the recent assignment of corresponding modes in the experimental spectra,[6,8,9] again confirming the validity of normal-mode analysis. Our SO_3 deformation frequencies, $\delta_s(SO_3)$ and $\delta_{as}(SO_3)$ modes, support the assignment of Meyer et al., who utilized an accurate investigation with the isotope effect, and assigned the lower frequency to $\delta_{as}(SO_3)$ not the $\delta_s(SO_3)$ mode.[6]

Structural and Dynamical Properties of the Hydration Shell. As for other polyatomic solutes, the fundamental information for a further analysis is the atomic RDFs.[31,33,49] We summarized the position of the first peak and its boundary for (site)$\cdots O_{water}$ and (site)$\cdots H_{water}$ RDFs in Table 3 for both ions. The evaluation of the atomic coordination numbers (CNs) utilizes the position of the atomic hydration boundary obtained from its (site)$\cdots O_{water}$ RDF, also listed in Table 3. According to the coincidence between the hydration shell of sulfur and three oxygen atoms in both ions within the radius of ~4.6 Å, we investigated all hydration properties without the inclusion of the sulfur atom to reduce the complexity of solutes. The smaller effect of the sulfur atom is reflected in a similar

dx.doi.org/10.1021/jp305648e | J. Phys. Chem. B 2012, 116, 11498−11507

Table 3. Characteristic Values of the Radial Distribution Function $g_{\alpha\beta}(r)$ for Each Site of Bisulfite and Sulfonate Anions in the Hydration Shell Determined by the QMCF MD Simulations

coordinating site	$r_{max}(O_w)^a$	$r_{min}(O_w)^a$	$r_{max}(H_w)^a$	$r_{min}(H_w)^a$	n^a
		SO_3H^-			
S	3.96	4.62	3.04	3.70	
O(1)	2.70	3.48	1.76	2.40	2.6
O(2)	2.72	3.54	1.78	2.50	2.9
O(3)	2.90	3.32	1.92	2.40	1.6
H	1.88, 2.08	2.68	2.50	2.66	0.7
molecular surface	2.72, 2.84	3.56	1.76, 1.88	2.64	6.5
		HSO_3^-			
S	3.94	4.58	3.04	3.86	
O(1)	2.84	3.68	1.92	2.58	2.7
O(2)	2.68, 2.90	3.58	1.80	2.64	2.4
O(3)	2.78, 2.94	3.38	1.86, 2.00	2.74	1.9
H	2.26	2.48	2.92	2.98	0.4
molecular surface	2.80, 2.88	3.68	1.88	2.74	6.6

[a] r_{max} and r_{min} are the distances of the maximum and minimum of $g_{\alpha\beta}(r)$ for the hydration shell in Å, and n is the averaged coordination numbers of the shell, respectively.

hydration shell in both ions, showing in the atomic S···O_{water} and S···H_{water} RDFs. The atomic RDFs of oxygen atoms in both ions represent a similar interaction with the water molecules, whereas the hydration shell of hydrogen atom in the bisulfite is stronger than that in the sulfonate ion. This agrees with the vibration analysis in the previous section. A difference of atomic hydrogen CNs reveals a slightly stronger interaction with the hydration shell of the bisulfite ion, which is in good agreement with the experimental[8,10] and theoretical[15−17] findings. However, only atomic properties are unsuitable to compare with experimental data, and hence, we also evaluated the molecular RDFs and CNDs of the hydration shells based on the molecular domain.[38] The molecular RDFs provide the possibility to find water molecules in the isotropic molecular domain constructed from the union of spheres having identical radii, by assigning the coordinating site with the shortest distance among the values obtained from the oxygen of water and each site within the solute. Parts a and b of Figure 10 present the molecular RDFs of bisulfite and sulfonate ions, respectively, showing a well-defined and similar hydration structure. The (molecular)···O_{water} RDF of bisulfite ion again reveals a slightly stronger interaction with water at the hydrogen site (a weak band at 1.36−2.34 Å) than that of the sulfonate ion (a weak band at 1.56−2.40 Å). Parts c and d of Figure 10 show the molecular CNDs of bisulfite and sulfonate ion, respectively, evaluated with the molecular domain, constructed by applying the boundary obtained from the atomic RDFs for each site of the solute.[38] The possible CNs of bisulfite are in a range of 4−9 with a dominant value of 7, while the molecular CND of sulfonate prefers 6 as the main CN with a higher flexibility of the hydration shell ranging from 4 to 11. The characteristic values of molecular hydration shells and their average CNs from the molecular RDFs and CNDs are also listed in Table 3. The higher CNs of bisulfite (7.8) and sulfonate (7.4) ions from the direct sum of atomic CNs than in the corresponding molecular CN, differing by 1.3 and 0.8 molecules, indicate the location of waters in the intersection volumes of the atomic hydration spheres. The visualization of the hydration shell during the simulation period provides an insight to understand the motion of water molecules around the solute. We again applied the contravariant transformation for the 3D alignment on the coordinates of solute and one selected water molecule within its molecular hydration shell, illustrating a motion of the solvent shown in Figure 11. The water molecule within the molecular hydration shell rapidly changes the coordinating site around the solutes during the simulation period, obviously supporting the statement in previous studies.[26,31,33,49] This is the evidence that the total atomic CNs include an overcounting of some water molecules, migrating around many coordinating sites during the simulation period.

According to the dynamical change of the water molecules across the coordinating sites, the number of actual contacts

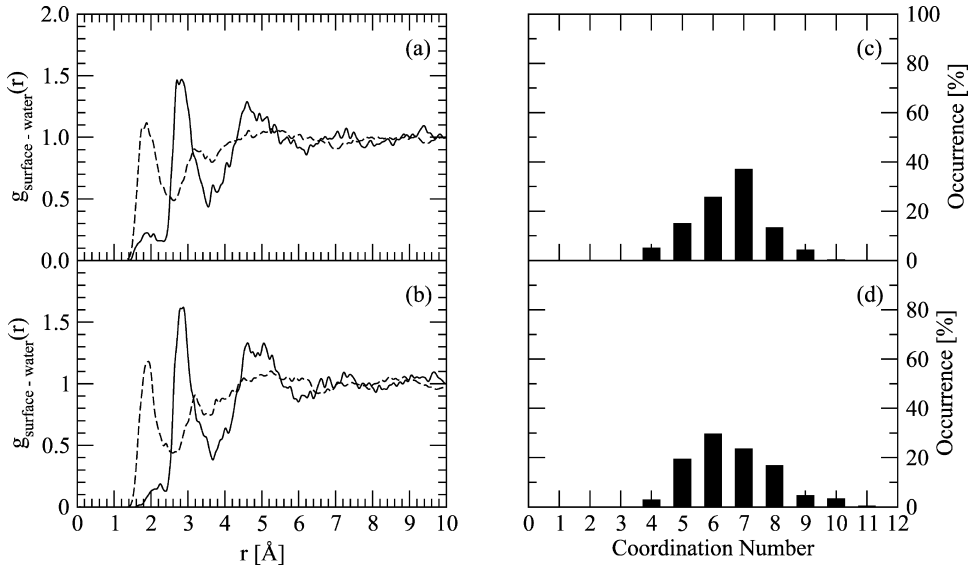

Figure 10. Molecular RDF plots of (a) SO_3H^- and (b) HSO_3^- anions obtained from the QMCF MD simulations evaluated by means of the molecular domain; solid and dashed lines refer to the RDFs for the O and H atoms of water, respectively. The molecular hydration shell coordination number distribution of (c) SO_3H^- and (d) HSO_3^- anions.

dx.doi.org/10.1021/jp305648e | J. Phys. Chem. B 2012, 116, 11498−11507

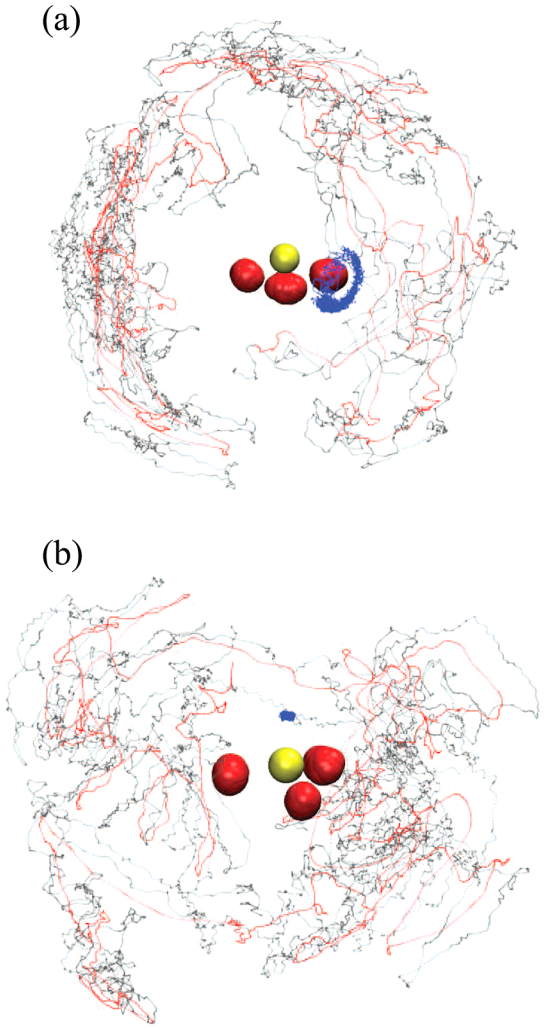

Figure 11. All superimposed trajectories for the coordinates of one selected water molecule in the molecular hydration shell for (a) bisulfite (SO_3H^-) and (b) sulfonate (HSO_3^-) ions with 3D alignment obtained from the QMCF MD simulations. The yellow sphere is sulfur, red spheres are oxygen of solutes, blue points are hydrogens of solutes, red dots are oxygens of the selected water molecules, and gray dots are the hydrogen atoms of the water.

based on the H-bonds determines the CNs and some extra waters in the H-bonds network between the hydration shell and bulk.[33,49] We utilized the structural criterion depending on the cutoff parameters in analogy to water−dimethyl sulfoxide[47] and our previous studies.[33,49] The cutoff distances $R_{OO}^{(c)}$ and $R_{HO}^{(c)}$ for each coordinating site correspond to the boundary of atomic hydration shells obtained from (site)···O_{water} and (site)···H_{water} RDFs, respectively. The angle $\varphi^{(c)}$ was set to 30°.[47] Table 4 lists the average number of H-bonds for each site and the molecular hydration (surface) of the SO_3H^- and HSO_3^- ions. The average H-bonds of the surface were evaluated by averaging the summation of all H-bonds in each time step over the simulation period. The equivalence between the total of each site and the surface values presents the ratio 1:1 for the formation of an H-bond between the water molecule and the coordinating site, resulting in the actual CN for bisulfite (5.3) and sulfonate (5.0) ions. The comparison for these H-bond data with the molecular CNDs (6.5 and 6.6 for the bisulfite and sulfonate ion, respectively) specifies some extra water molecules located in the molecular hydration shell of bisulfite (1.2) and sulfonate (1.6) ion without forming the direct interaction to the solutes, readily changing the coordinating sites and connecting with bulk. The smaller number of extra water for bisulfite also indicates a stronger hydration structure than that of the sulfonate ion, in good agreement with previous experimental[10] and theoretical[15−17] conclusions.

A further dynamical property of water molecules within the hydration shell was investigated by the ligand MRT calculated by the direct method,[39] dividing the average number of water molecules within the hydration shell throughout the simulation period by the number of exchange events with two time parameters (t^* = 0.0 and 0.5 ps) corresponding to all displacements and to sustainable exchange events.[41] MRT values for all coordinating sites and molecular hydration shell for both ions are summarized in Table 5, compared with the data of pure water simulations.[39,40] The number of involved ligands (N_{inv}) represents the coordination of water molecules with the evaluated site in the criterion of t^*, while the number of accounted exchange events (N_{ex}) accumulates the exchange process of N_{inv} throughout the simulation period. The standard relaxation time utilized in the direct method with t^* = 0.5 ps leads to the MRT of water ligands at the coordinating sites, while the hydrogen bond liftimes can be estimated with t^* = 0.0 ps.[31,39] The total number of individual N_{inv} of sulfonate evaluated by t^* = 0.5 ps is larger than that of bisulfite ion, whereas the molecular values present the reverse order. This again indicates a higher degree of overcounting for each coordinating site of sulfonate than of bisulfite ion. The difference value between the total atomic $N_{ex}^{0.5}$ and the molecular $N_{ex}^{0.5}$ suggests that the migrations of water molecules between the coordinating sites were 14 and 24 processes for bisulfite and sulfonate ion, respectively. The number of migrations for the water among the coordinating sites within the sulfonate ion is larger than its molecular $N_{ex}^{0.5}$ (18), representing the confined waters within the molecular hydration shell and reflecting a longer MRT of the molecular hydration shell of the sulfonate than of the bisulfite ion. Our MRT results compared with the simulations data of pure water[39,40] classify the bisulfite as a structure-making ion, while the sulfonate ion shows more complex properties due to the zero of $N_{inv}^{0.5}$ and $N_{ex}^{0.5}$ values of the hydrogen atom. The atomic MRTs of oxygen atoms within the sulfonate ion show a similar property with the pure water, whereas the value of hydrogen atom indicates that it is not involved in any H-bond agreeing with the data reported by Steudel et al.[48] However, the molecular MRT of sulfonate ion reveals a stronger hydration structure than the pure water, thus we also classify it as a

Table 4. Average Number of Hydrogen Bonds for Each Coordinating Site and Molecular Surface of SO_3H^- and HSO_3^- Anions in the Simulation Period

	O(1)	O(2)	O(3)	H	surface
SO_3H^-	2.0 ± 0.7	2.1 ± 0.7	0.7 ± 0.6	0.5 ± 0.5	5.3 ± 1.1
HSO_3^-	1.7 ± 0.6	1.6 ± 0.6	1.5 ± 0.6	0.2 ± 0.4	5.0 ± 1.1

dx.doi.org/10.1021/jp305648e | J. Phys. Chem. B 2012, 116, 11498−11507

Table 5. Mean Ligand Residence Time t (ps), Number of Accounted Ligand Exchange Events N and Total Number of Processes Needed for One Successful Water Exchange R_{ex} Obtained from the QMCF MD Simulations

	t^* = 0.0 ps			t^* = 0.5 ps			
	N_{inv} [a]	$N_{ex}^{0.0}$/10 ps [b]	$\tau_D^{0.0}$ [c]	N_{inv} [a]	$N_{ex}^{0.5}$/10 ps [b]	$\tau_D^{0.5}$ [c]	R_{ex} [d]
			SO_3H^-				
O(1)	18	95	0.28	8	14	1.88	6.8
O(2)	22	136	0.22	8	13	2.28	10.5
O(3)	20	141	0.12	5	10	1.67	14.1
H	11	99	0.07	1	3	2.37	33.0
surface	34	417	0.15	15	26	2.46	16.0
			HSO_3^-				
O(1)	21	118	0.23	10	18	1.52	6.6
O(2)	20	120	0.20	8	14	1.72	8.6
O(3)	15	84	0.23	7	10	1.93	8.4
H	6	57	0.06	0	0	0.00	–
surface	29	258	0.25	13	18	3.38	14.3
			Pure Water				
H_2O [e]		269[39]	0.2,[39] 0.33[40]		24[39]	1.7,[39] 1.51[40]	11.2[39]
H_2O		131[f]	0.2,[f] 0.55[41]		20[f]	1.3[f]	6.5[f]

[a]Number of ligands involved in the MRT evaluation according to the value of t^*. [b]Number of accounted exchange events per 10 ps lasting at least 0.0 and 0.5 ps, respectively. [c]Mean residence time determined by the direct method[39] in picoseconds. [d]Average number of processes needed for one successful ligand exchange. [e]Values obtained from a QM/MM-MD simulation of pure water[39,40] in picoseconds. [f]Unpublished results: values obtained from a QMCF MD simulation of pure water in picoseconds.

structure-maker consisting of three hydrophilic S−O and one hydrophobic S−H bonds. The number of processes needed for one successful water exchange, R_{ex}, being the ratio of $N_{ex}^{0.0}$ to $N_{ex}^{0.5}$ also shows a complexity of the exchange process. The R_{ex} for the interchanging of coordinating site within the molecular hydration shell was 3.8 and 5.0 for bisulfite and sulfonate ion, respectively, indicating a higher reactivity of the coordinating sites within the former than those of the latter.

CONCLUSION

Vibrational investigations based on the precise assignment of normal modes for the aqueous bisulfite and sulfonate ions were performed on the basis of the data obtained from the QMCF MD simulations. The complexity of C_1 symmetry for the bisulfite ion was simplified with (SO_2), $(SO_2)-(O^*)$, and $(SO_2O)-(H)$ models, providing the data for all nine modes. All six normal modes of sulfonate ion were also evaluated to compare with the experimental data. Here, the vector analysis gave the frequency of $\delta_s(SO_3)$ lower than that of the $\delta_{as}(SO_3)$ mode, which is in a good agreement with the assignment in accurate experimental data.[6] The S−H bond in the sulfonate ion displays a hydrophobic property as it presents a stronger bond and shorter distance when a water molecule comes close to the hydrogen atom, reflected in a blue-shifted peak of the ν(SH) mode. The superimposed trajectories of the atomic coordinates for the solutes with 3D alignment, presenting the possibility of bisulfite ion to arrange a suitable orientation of the active hydrogen atom to form the *trans*-SO_3H^- conformer, support the proposed mechanism for the tautomerization from the bisulfite to sulfonate ion.[17] Unfortunately, the isomerization was not observed in this work, due to the short time-span of simulation. We illustrated the migration of water molecules within the molecular hydration shell among coordinating sites of the solutes, confirming related statements in previous studies of hydrated anions.[26,31,33,49] The investigated properties of vibrations and hydration shells in this study indicate more stability of the sulfonate than the bisulfite ion in aqueous solution, while the former has a weaker hydration structure than the latter ion. Our results provided the characteristics of the specified ions in a separated system that is difficult to realize in experiment, due to the coexistance of bisulfite and sulfonate ions in equilibrium in the prepared solutions.[8,10]

AUTHOR INFORMATION

Corresponding Author

*Viwat.V@Chula.ac.th

Notes

The authors declare no competing financial interest.

ACKNOWLEDGMENTS

Financial support by ASEA-UNINET, the National Research University (NRU) Project of Thailand's Office of the Higher Education Commission, and Centre for Petroleum, Petrochemicals and Advanced Materials, Chulalongkorn University are gratefully acknowledged. A.T. acknowledges support by the Thailand Research Fund (TRF) and Suranaree University of Technology (SUT). This work was also supported by the National Research Council of Thailand (NRCT) and the commission of Higher Education (CHE) of Thailand.

REFERENCES

(1) Brandt, C.; van Eldik, R. *Chem. Rev.* **1995**, *95*, 119−190.
(2) Bakker, J.; Clarke, R. J. *Wine Flavour Chemistry*, 2nd ed.; Blackwell Publishing: West Sussex, UK, 2012.
(3) Golding, R. M. *J. Chem. Soc.* **1960**, 3711−3716.
(4) Herlinger, A. W.; Long, T. V. *Inorg. Chem.* **1969**, *8*, 2661−2665.
(5) Connick, R. E.; Tam, T. M.; Von Deuster, E. *Inorg. Chem.* **1982**, *21*, 103−107.
(6) Meyer, B.; Peter, L.; Shaskey-Rosenlund, C. *Spectrochim. Acta, Part A* **1979**, *35*, 345−354.
(7) Zhang, Z.; Ewing, G. E. *Spectrochim. Acta, Part A* **2002**, *58*, 2105−2113.
(8) Risberg, E. D.; Eriksson, L.; Mink, J.; Pettersson, L. G. M.; Skripkin, M. Y.; Sandström, M. *Inorg. Chem.* **2007**, *46*, 8332−8348.
(9) Townsend, T. M.; Allanic, A.; Noonan, C.; Sodeau, J. R. *J. Phys. Chem. A* **2012**, *116*, 4035−4046.

(10) Horner, D. A.; Connick, R. E. *Inorg. Chem.* **1986**, *25*, 2414−2417.
(11) Baird, N. C.; Taylor, K. F. *J. Comput. Chem.* **1981**, *2*, 225−230.
(12) Strömberg, A.; Gropen, O.; Wahlgren, U.; Lindqvist, O. *Inorg. Chem.* **1983**, *22*, 1129−1133.
(13) Squires, R. R. *Int. J. Mass Spectrom. Ion Processes* **1992**, *117*, 565−600.
(14) Smith, A.; Vincent, M. A.; Hillier, I. H. *J. Phys. Chem. A* **1999**, *103*, 1132−1139.
(15) Brown, R. E.; Barber, F. *J. Phys. Chem.* **1995**, *99*, 8071−8075.
(16) Otto, A.; Steudel, R. *Eur. J. Inorg. Chem.* **2000**, 617−624.
(17) Voegele, A. F.; Tautermann, C. S.; Rauch, C.; Loerting, T.; Liedl, K. R. *J. Phys. Chem. A* **2004**, *108*, 3859−3864.
(18) Rode, B. M.; Hofer, T. S.; Randolf, B. R.; Schwenk, C. F.; Xenides, D.; Vchirawongkwin, V. *Theor. Chem. Acc.* **2006**, *115*, 77−85.
(19) Hofer, T. S.; Pribil, A. B.; Randolf, B. R.; Rode, B. M. Ab Initio Quantum Mechanical Charge Field Molecular Dynamics: A Non-parametrized First-Principle Approach to Liquids and Solutions. In *Combining Quantum Mechanics and Molecular Mechanics. Some Recent Progresses in QM/MM Methods*; Sabin, J. R., Brändas, E., Eds.; Academic Press: New York, 2010; Vol. *59*, pp 213−246.
(20) Warshel, A.; Levitt, M. *J. Mol. Biol.* **1976**, *103*, 227−249.
(21) Field, M. J.; Bash, P. A.; Karplus, M. *J. Comput. Chem.* **1990**, *11*, 700−733.
(22) Gao, J. *J. Am. Chem. Soc.* **1993**, *115*, 2930−2935.
(23) Bakowise, D.; Thiel, W. *J. Phys. Chem.* **1996**, *100*, 10580−10594.
(24) Brooks, B. R.; Bruccoleri, R. E.; Olafson, B. D.; States, B. D.; Swaminathan, S.; Karplus, M. *J. Comput. Chem.* **1983**, *4*, 187−217.
(25) Berendsen, H. J. C.; Postma, J. P. M.; van Gunsteren, W. F.; DiNola, A.; Haak, J. R. *J. Chem. Phys.* **1984**, *81*, 3684−3690.
(26) Vchirawongkwin, V.; Rode, B. M.; Persson, I. *J. Phys. Chem. B* **2007**, *111*, 4150−4155.
(27) Vchirawongkwin, V.; Rode, B. M. *Chem. Phys. Lett.* **2007**, *443*, 4152−157.
(28) Pribil, A. B.; Vchirawongkwin, V.; Hofer, T. S.; Randolf, B. R. Structure and Dynamics of Composite Anions in Aqueous Solution. *Computation in Modern Science and Engineering, Proceedings of the International Conference on Computational Methods in Science and Engineering* **2007**, 921−923.
(29) Pribil, A. B.; Hofer, T. S.; Randolf, B. R.; Rode, B. M. *J. Comput. Chem.* **2008**, *29*, 2330−2334.
(30) Pribil, A. B.; Hofer, T. S.; Vchirawongkwin, V.; Randolf, B. R.; Rode, B. M. *Chem. Phys.* **2008**, *346*, 182−185.
(31) Vchirawongkwin, V.; Pribil, A. B.; Rode, B. M. *J. Comput. Chem.* **2010**, *31*, 249−257.
(32) Vchirawongkwin, V.; Kritayakornupong, C.; Ruangpornvisuti, V.; Rode, B. M. *J. Mol. Struct. (THEOCHEM)* **2009**, *913*, 236−239.
(33) Vchirawongkwin, V.; Kritayakornupong, C.; Rode, B. M. *J. Phys. Chem. B* **2010**, *114*, 11561−11569.
(34) Dunning, Jr., T. H.; Hay, P. J. In *Gaussian Basis Sets for Molecular Calculations*; Schaefer, H. F., III, Ed.; Plenum Press: New York, 1977; Vol. *3*, Chapter 1, pp 1−27.
(35) Dunning, T. H., Jr. *J. Chem. Phys.* **1970**, *53*, 2823−2833.
(36) Stillinger, F. H.; Rahman, A. *J. Chem. Phys.* **1978**, *68*, 666−670.
(37) Bopp, P.; Janscó, G.; Heinzinger, K. *Chem. Phys. Lett.* **1983**, *98*, 129−133.
(38) Vchirawongkwin, S.; Vchirawongkwin, V. *Comput. Theor. Chem.* **2011**, *974*, 26−30.
(39) Hofer, T. S.; Tran, H. T.; Schwenk, C. F.; Rode, B. M. *J. Comput. Chem.* **2004**, *25*, 211−217.
(40) Xenides, D.; Randolf, B. R.; Rode, B. M. *J. Chem. Phys.* **2005**, *122*, 174−506.
(41) Lock, A. J.; Woutersen, S.; Bakker, H. J. *J. Phys. Chem. A* **2001**, *105*, 1238−1243.
(42) Bopp, P. *Chem. Phys.* **1986**, *106*, 205−212.
(43) Eklund, L.; Hofer, T. S.; Pribil, A. B.; Rode, B. M.; Persson, I. *Dalton Trans.* **2012**, *41*, 5209−5216.
(44) Curtiss, L. A.; Redfern, P. C.; Raghavachari, K.; Rassolov, V.; Pople, J. A. *J. Chem. Phys.* **1999**, *110*, 4703−4709.
(45) Frisch, M. J.; et al. *Gaussian03*, Revision D.02; Gaussian, Inc., Wallingford, CT, 2004.
(46) Noblet, J. A.; Schugart, K. A. *J. Mol. Struct. (THEOCHEM)* **1994**, *304*, 1−11.
(47) Luzar, A.; Chandler, D. *J. Chem. Phys.* **1993**, *98*, 8160−8173.
(48) Steudel, R.; Steudel, Y. *Eur. J. Inorg. Chem.* **2009**, *2009*, 1393−1405.
(49) Vchirawongkwin, V.; Kritayakornupong, C.; Tongraar, A.; Rode, B. M. *J. Phys. Chem. B* **2011**, *115*, 12527−12536.